Susceptibility, magnetization and Mössbauer studies of the Mg–Zn ferrite system

H. H. JOSHI, R. G. KULKARNI
Department of Physics, Saurashtra University, Rajkot-360 005, India

The variation of susceptibility with temperature of the $Zn_xMg_{1-x}Fe_2O_4$ system has been obtained between 300 K and the Neél temperature at a constant magnetic field of 7.0 Oe for $x = 0.0$ to 0.7. Through the magnetization measurements of this Mg–Zn ferrite system the variation of saturation magnetization with zinc concentration was determined in gaining information about the Yafet–Kittel angles in the system for $x \leqslant 0.9$ at 298 K. The observations indicate the existence of a Yafet–Kittel type of magnetic ordering in the system. A molecular field analysis of the Y–K spin ordering using a three sublattice model is shown to explain the experimental data satisfactorily. For the sake of verification, Neél temperatures of Mg–Zn ferrites were also determined from Mössbauer studies.

1. Introduction

Most of the zinc substituted ferrites like Ni–Zn [1], Fe–Zn [2] and Cu–Zn [3] show a canted spin arrangement on the octahedral or B-site. The canting of the spins gives rise to Yafet–Kittel angles (Y–K), which suggests that A–B and B–B superexchange interactions are comparable in strength. Practically no information exists about the magnetic properties and magnetic ordering of the Mg–Zn ferrite system for varying zinc concentrations except for our recent Mössbauer studies at 77 and 298 K [4, 5].

The present paper reports magnetization, susceptibility and a Mössbauer study of Mg–Zn ferrites at various zinc concentrations. The magnetization measurements were primarily undertaken to investigate the variation of the saturation magnetization with zinc concentration and to gain information about the Y–K angles in the system. A molecular field analysis of the Y–K spin ordering using three sublattice models is shown to explain the experimental data satisfactorily. The variation of low field a–c susceptibility with temperature of Mg–Zn ferrites was studied to determine the Neél temperatures and to find the magnetic ordering.

The temperature dependence of Mössbauer spectra was obtained to verify the Neél temperatures obtained from susceptibility measurements and to study the variation of hyperfine field with temperature.

2. Experimental details

Eleven samples of $Zn_xMg_{1-x}Fe_2O_4$ system with $x = 0.0, 0.1, 0.2, 0.3, 0.4, 0.5, 0.6, 0.7, 0.8, 0.9$ and 1.0 were prepared by the usual ceramic method, from pure Fe_2O_3, MgO and ZnO powders. The oxides were mixed in stoichiometric proportions and fired at 1100° C for 50 h and slowly cooled to room temperature.

The X-ray powder diffractometry results of all compositions clearly indicated the presence of only the cubic spinel phase with no extra lines corresponding to any other phase. The X-ray powder diffractometry patterns were recorded on a Philips diffractometer using $FeK\alpha$ radiation.

The a–c susceptibility measurements on powdered samples were made in a temperature range 300 to 800 K using a double coil set-up [6] operating at a frequency of 263 Hz and in a r.m.s. field of 7.0 Oe.

The saturation magnetization of each sample was carried out using the high-field hysteresis loop technique described elsewhere [7].

The Mössbauer spectrometer was equipped with a source of 10 mCi ^{57}Co(Pd). The experimental set-up has been described in our earlier work [8]. The Mössbauer spectra of $Zn_xMg_{1-x}Fe_2O_4$ for $x = 0.0$ to 0.7 were obtained at different temperatures between 300 K and the Neél temperatures.

3. Results and discussion

By means of Mössbauer results [4] and X-ray diffraction of Mg–Zn ferrites the cation distribution has been found to be $(Zn_x^{2+}Fe_{1-x}^{3+})^A[Mg_{1-x}^{2+}Fe_{1+x}^{3+}]^BO_4^{2-}$, where the ions enclosed by the round brackets correspond to tetrahedral or A-site and the ions enclosed by the square brackets correspond to octahedral or B-site.

3.1. Lattice constant and density

The variation of lattice constant with zinc content for $Zn_xMg_{1-x}Fe_2O_4$ is shown in Fig. 1. The lattice constant increases linearly from $MgFe_2O_4$ to $ZnFe_2O_4$, which is due to the larger ionic radius of Zn^{2+} (0.074 nm) which, when substituted for the divalent metal ion in the lattice, replaces the smaller Fe^{3+} (0.06 nm) ion on the A-site. No previous measurements of lattice constants exist in the literature for Mg–Zn ferrites at different values of zinc content. The X-ray densities of all the samples have been calculated from molecular weight and volume of the unit cell and values are given in Table I. The X-ray density increases
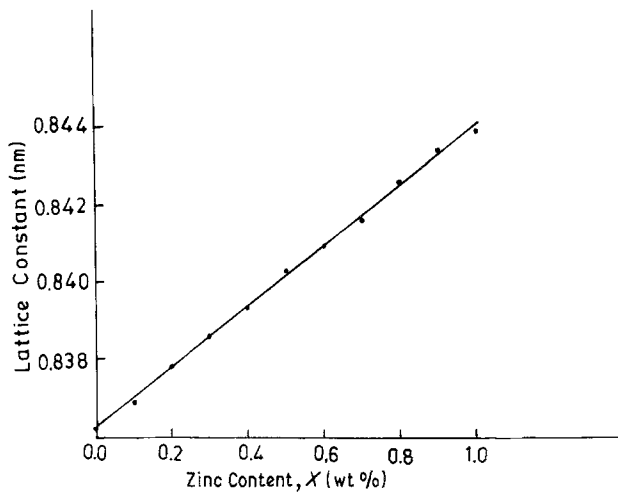
Figure 1 Variation of the lattice constant for $Zn_xMg_{1-x}Fe_2O_4$ system as a function of zinc content (x).

with x, which suggests that the increase in mass overtakes the increase in volume of the unit cell with zinc substitution.

3.2. Susceptibility

The typical plots of relative low field $a-c$ susceptibility against temperature are shown in Fig. 2, which exhibits normal ferrimagnetic behaviour. The Neél temperatures determined from Fig. 2 are listed in Table I. It is apparent from Table I that there is a sharp decrease in Neél temperature for small additions of zinc. This is due to the decreasing $A-B$ interactions resulting from replacement of Fe^{3+} by Zn^{2+} on A-sites.

3.3. Magnetization

The field dependence of magnetization obtained at 298 K is shown in Fig. 3. From Fig. 3 the values of saturation magnetization have been estimated within an accuracy of about 5% and are listed in Table I. The magneton number i.e. saturation magnetization per formula unit in Bohr magneton (n_B) at 298 K initially increases and then decreases as x is increased.

A similar variation of n_B with x has also been observed in other zinc substituted ferrites [1–3], which has been attributed to the presence of Yafet–Kittel angles in the spin system on B-sites. On account of similarities between Mg–Zn and other zinc substituted
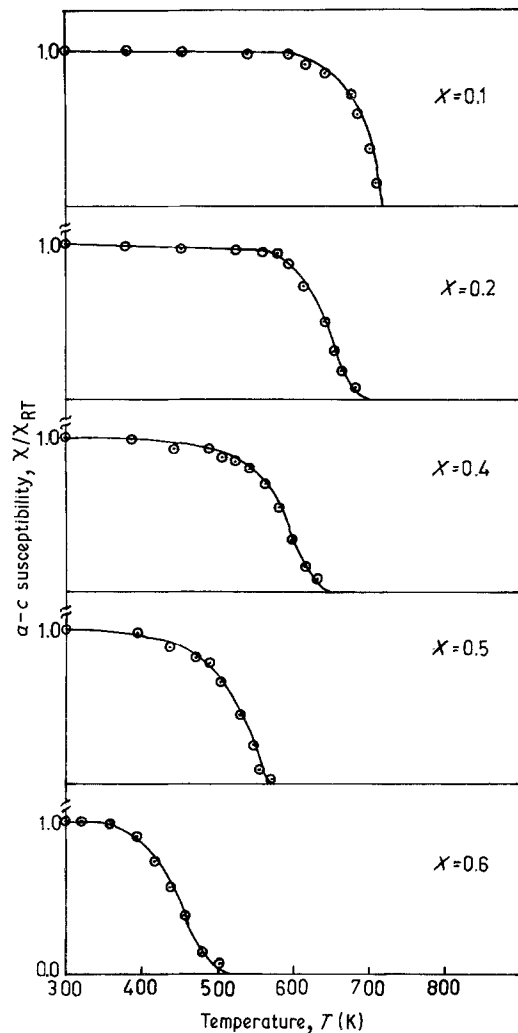

Figure 2 The temperature dependence of relative low field $a-c$ susceptibility (χ/χ_{RT}) for $Zn_xMg_{1-x}Fe_2O_4$ system. (χ/χ_{RT}) is the ratio of susceptibility (χ) at temperature T, to susceptibility at room temperature χ_{RT}.

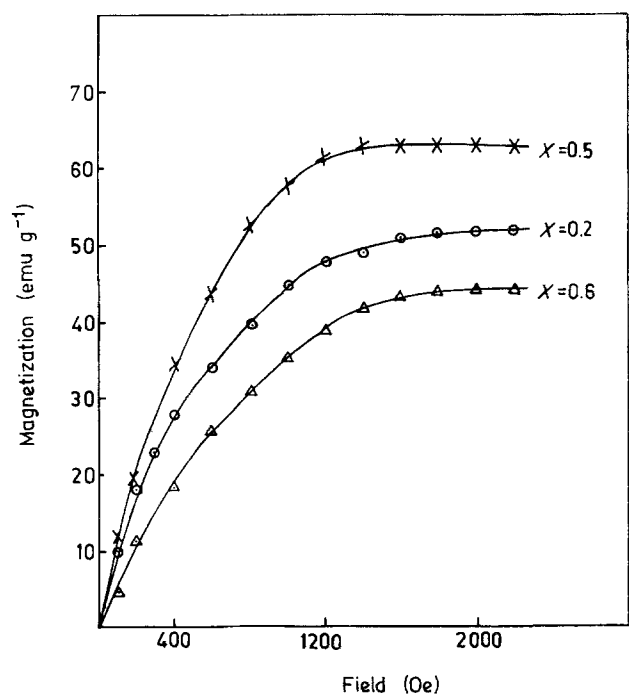TABLE I The X-ray density ϱ, saturation magnetization σ_s, and Neél temperature T_N for $Zn_xMg_{1-x}Fe_2O_4$

x	ϱ (g cm^{-3})	σ_s (emu g^{-1}) 298 K	T_N (K) Susceptibility	T_N (K) Mössbauer
0.0	4.55	26	730	723
0.1	4.63	40	715	700
0.2	4.71	52.	670	660
0.3	4.79	58	630	620
0.4	4.87	62	610	593
0.5	4.94	63	540	523
0.6	5.02	44	480	470
0.7	5.10	21	370	353
0.8	5.17	8	—	—
0.9	5.25	3	—	—
1.0	5.33	—	—	—

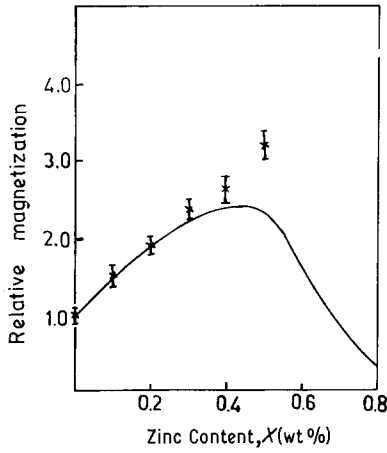*Figure 3* Field dependence of magnetization for the Mg–Zn ferrite system at 298 K.

Figure 4 The relative saturation magnetization per formula unit at 298 K for Mg–Zn ferrites as determined from Equation 1 using Mössbauer data. The solid line represents data from magnetization measurements. ($\ddagger$) Mössbauer; (−) magnetization.

TABLE II Saturation magnetization per formula unit in Bohr magneton at 298 K. The values of the exchange constants in K used in calculating α_{YK} are as follows: $J_\beta = -13.5$ K and $J_\delta = -10$ K

x	n_B	Yafet–Kittel angle (α_{YK})	
		Calculated	Experimental
0.0	0.93	0°	0°
0.1	1.45	0°	0°
0.2	1.97	0°	0°
0.3	2.21	0°	0°
0.4	2.39	0°	3° 29'
0.5	2.47	25° 50'	25° 22'
0.6	1.77	47° 33'	47° 41'
0.7	0.86	61° 35'	65° 33'
0.8	0.33	72° 32'	76° 45'
0.9	0.13	81° 52'	83° 52'

ferrites it is reasonable to assume that Yafet–Kittel angles are also present in the former system.

An indirect check for the presence of a canted spin structure follows from the apparent proportionality between average hyperfine field $|H|$ and the average sublattice magnetization. It can be shown that

$$\mu(x) = \frac{|H_B(x)|}{|H_B(0)|}[(1 + x)\mu(Fe^{3+})$$
$$+ (1 - x)\mu(Mg^{2+})]$$
$$- \frac{|H_A(x)|}{|H_A(0)|}[(1 - x)\mu(Fe^{3+})] \qquad (1)$$

where, $\mu(x)$ is the magnetic moment per formula unit $(Zn_x^{2+}Fe_{1-x}^{3+})^A[Mg_{1-x}^{2+}Fe_{1+x}^{3+}]^BO_4^{2-}$, $\mu(Fe^{3+})$ and $\mu(Mg^{2+})$ are the ionic moments of Fe^{3+} and Mg^{2+}, $|H_B(x)|$ and $|H_A(x)|$ are the magnitudes of average nuclear magnetic fields for the octahedral and tetrahedral Fe^{3+} ions, respectively. The ionic magnetic moment of Mg^{2+} is zero, but because of partial inversion (90%) of $MgFe_2O_4$ structure, the magnetic moments of A and B-sites are $4.5\,\mu_B$ and $5.5\,\mu_B$, respectively. It is assumed that the relative magnetization $\sigma(x)/\sigma(x = 0)$ at 298 K is $\mu(x)/\mu(x = 0)$. The values of relative magnetization $\sigma(x)/\sigma(x = 0)$ as a function of x were determined from Equation 1 using the values of hyperfine fields and distribution of Fe^{3+} ions on A- and B-sites at 298 K from Mössbauer data [5]. The results are depicted in Fig. 4. The agreement between $\sigma(x)/\sigma(x = 0)$ as calculated from Equation 1 and $\sigma(x)/\sigma(x = 0)$ as measured from magnetization measurements at 298 K is quite good for $x \leqslant 0.4$ but becomes increasingly worse as x increases above 0.4. This behaviour can be interpreted as indirect evidence for the presence of canted spin structure because the Mössbauer effect measures the magnitude of $\langle S_z \rangle$, while the macroscopic magnetization depends on the component of $\langle S_z \rangle$ parallel to the external field. The discrepancy between the magnetization measurement and Mössbauer data can be taken as an indirect evidence for the presence of Yafet–Kittel angles.

The condition for the existence of Y–K angles to occur in the Ni–Zn system has been investigated in

the molecular field approximation by Satya Murthy *et al.* [9] using a non-colinear three sublattice model. On a similar basis we can write the interaction energy involving the Y–K angles for the Mg–Zn ferrite system as

$$E_{YK} = [25(1 - x^2)\beta]\cos\alpha_{YK}$$
$$- \tfrac{1}{4}[25(1 + x)^2\,\delta]\cos 2\alpha_{YK} \qquad (2)$$

The terms β and δ are the molecular field constants related to the following exchange interactions

$$\beta : A(Fe^{3+}) \longrightarrow B_i(Fe^{3+})$$
$$\delta : B_1(Fe^{3+}) \longrightarrow B_2(Fe^{3+}),$$
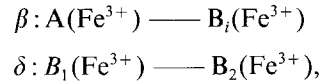
where, $i = 1, 2$.

The energy is minimum for (a) $\sin\alpha_{YK} = 0$, which corresponds to the Néel's configuration or for (b)

$$\cos\alpha_{YK} = \left(\frac{1 - x}{1 + x}\right)\beta/\delta \qquad (3)$$

which corresponds to the situation where the Y–K ordering is feasible. Here for example

$$\beta = \frac{2Z_{AB_i}J_\beta(Fe^{3+} \longrightarrow Fe^{3+})}{N_{B_i}g_Ag_{B_i}\mu_B^2} \qquad (4)$$

Where, J_β is the interaction between $A(Fe^{3+})$ and $B_i(Fe^{3+})$. Z_{AB_i} is the B_i nearest neighbours to A. N_{B_i} is the number of ions per unit formula. μ_B is the Bohr magneton and g denotes the Lande's splitting factor.

Adopting the procedure of Kulkarni and Patil [3] the following value of $J_\delta = -10.0$ K has been accepted for the $Zn_xMg_{1-x}Fe_2O_4$ system. Finally, we have estimated the value of J_β from the best fit for the variation of saturation magnetization with zinc concentration using the relation

$$n_B = (5 + x)\cos\alpha_{YK} - 5(1 - x) \qquad (5)$$

where n_B has been expressed in units of Bohr magneton. We have obtained $J_\beta = -13.5$ K.

Table II contains the experimental values of α_{YK} obtained from the observed variation of n_B with x using Equation 5 and the values calculated from Equation 3. From Table II it is clear that experimentally Y–K angles do not exist up to $x \leqslant 0.3$, but for $x \geqslant 0.4$, Y–K angles are present. There is a satisfactory agreement between the experimental and theoretical values of α_{YK} except for $x = 0.4$. Thus the
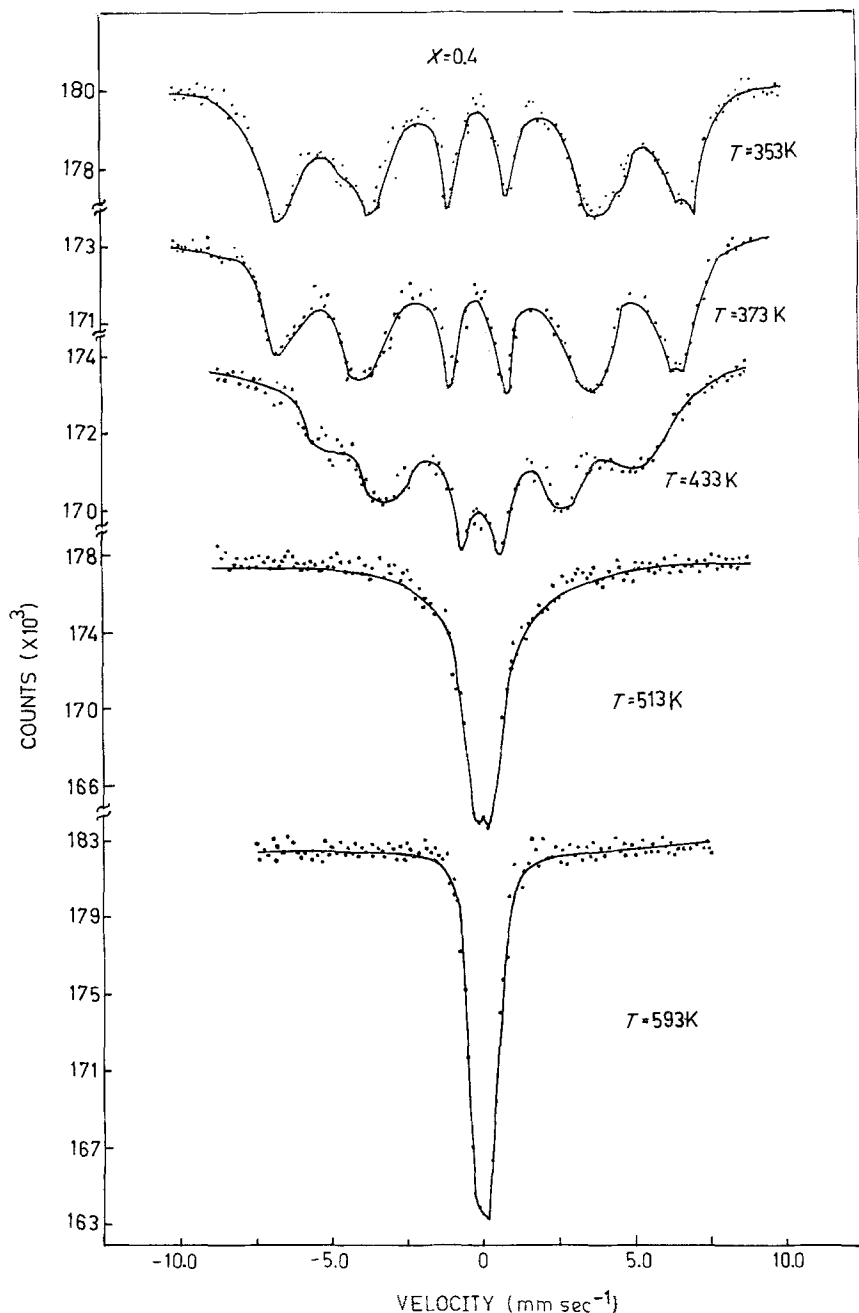
Figure 5 Mössbauer spectra of $Zn_{0.4}Mg_{0.6}Fe_2O_4$ at various temperatures.

X=0.4

T=353K

T=373 K

T=433 K

T=513K

T=593K

COUNTS (×10³)

VELOCITY (mm sec⁻¹)

observed variation of saturation magnetization with zinc has been explained on the basis of the existence of Y–K angles on B-site spins. This suggests that A–B and B–B superexchange interactions are comparable in strength.

3.4. Mössbauer study

The room temperature Mössbauer spectra [5] of the samples with x = 0.0 to 0.6 showed magnetic hyperfine patterns and the samples with x = 0.7 to 1.0 showed paramagnetic doublets only. The typical Mössbauer spectra of sample x = 0.4 at various temperatures are shown in Fig. 5. The Néel temperatures (T_N) determined by the stationary source and absorber method for x = 0.0 to 0.7 are given in Table I and these values are in very good agreement with the Néel temperatures obtained from susceptibility measurements. For $Zn_xMg_{1-x}Fe_2O_4$, T_N decreases with zinc content (x) and also the decrease is not linear (Fig. 6), this suggests that the exchange interaction decreases with increasing zinc concentration.

The plots of reduced hyperfine field $H(T)/H(0)$ against reduced temeprature T/T_N for both A- and B-sites (Fig. 7) follow the Brillouin function characteristic of iron with S = 5/2. From these plots it is clear that the magnetic fields (within the experimental error) are proportional to the sublattice magnetization.
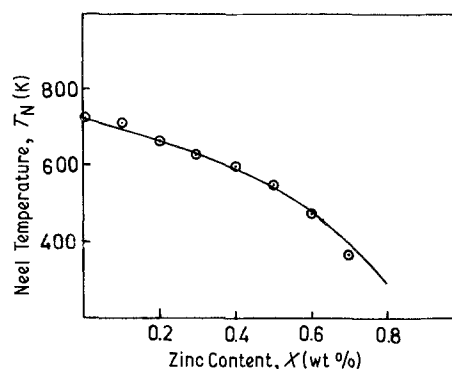
Néel temperature, T_N (K)

Zinc Content, X(wt %)

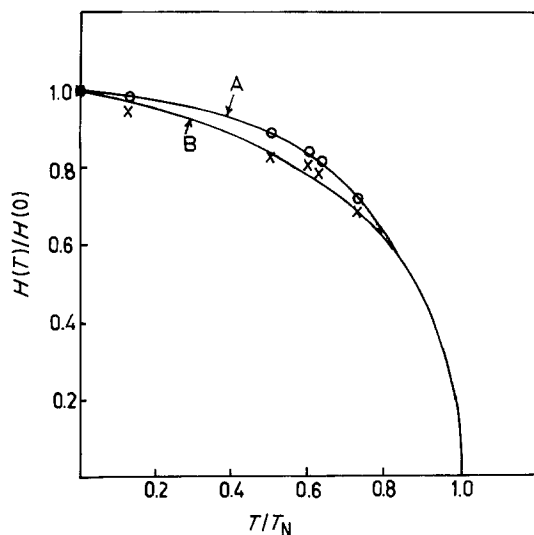*Figure 6* Variation of Néel temperature (T_N) for $Zn_xMg_{1-x}Fe_2O_4$ system with zinc content (x).

Figure 7 The reduced hyperfine field against reduced temperature for A and B-sites of $Zn_{0.4}Mg_{0.6}Fe_2O_4$. The full cuve is the Brillouin curve for $S = 5/2$.

Within the molecular field model it is predicted that in spinels the A-site ions are subjected to the stronger molecular field and therefore with increasing temperature it will be harder to disrupt the magnetic alignment in the A-sublattice than the B-sublattice. Hence the field at the tetrahedral site should have a slower variation with temperature than at the octahedral site. This explains why the B-site curve falls below the A-site one in Fig. 7. The log–log plot of the values (Fig. 8) shows straight lines for both A and B sites verifying the one-third power law [10], which describes the substances magnetization for samples with $0.0 \sim x \sim 0.5$.

The centre shifts (CS) are characteristic of the high spin Fe^{3+} charge state. The values of CS decrease with increase in temperature due to a second order Doppler effect (Table III). In our earlier work on this ferrite system [4, 5], no quadrupole splitting was observed for all magnetically split spectra but it was observed for paramagnetic doublets. It is evident from Table III that the quadrupole splitting (QS) is zero (within the
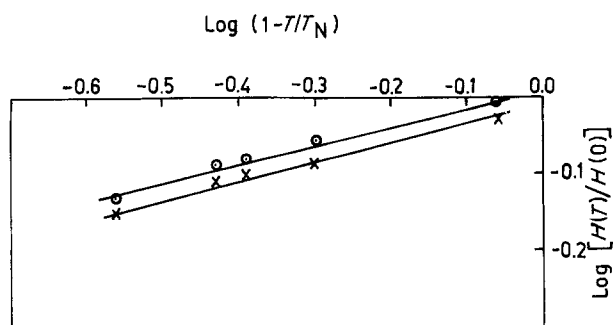

Figure 8 One-third power law as applied for sample $Zn_{0.4}Mg_{0.6}Fe_2O_4$. (⊙) A-site; (x) B-site.

TABLE III Temperature dependence of Mössbauer parameters for $Zn_{0.4}Mg_{0.6}Fe_2O_4$

T(K)	Centre shift* (mm sec^{-1})		Quadrupole splitting (mm sec^{-1})	
	CS(B)	CS(A)	QS(B)	QS(A)
4.2	0.60 ± 0.02	0.56 ± 0.02	0.00 ± 0.02	0.00 ± 0.02
77	0.52 ± 0.03	0.48 ± 0.02	0.00 ± 0.03	0.00 ± 0.02
298	0.38 ± 0.02	0.27 ± 0.02	0.00 ± 0.02	0.00 ± 0.02
353	0.34 ± 0.02	0.22 ± 0.02	0.00 ± 0.06	0.00 ± 0.06
373	0.31 ± 0.02	0.20 ± 0.02	0.00 ± 0.06	0.00 ± 0.06
433	0.27 ± 0.02	–	0.00 ± 0.06	0.00 ± 0.06
513	0.22 ± 0.02	–	0.38 ± 0.06	–
593	0.13 ± 0.02	–	0.32 ± 0.06	–
673	0.11 ± 0.02	–	0.27 ± 0.06	–

*With respect to iron metal.

experimental error) for all magnetically split spectra of $x = 0.4$ but it is present just below and above its Neél temperature. This may be attributed to the chemical disorder in this ferrite system.

References

1. L. K. LEUNG, B. J. EVANS and A. H. MORRISH, *Phys. Rev.* **B8** (1973) 29.
2. C. M. SRIVASTAVA, S. N. SHRINGI and R. G. SRIVASTAVA, *ibid.* **B14** (1976) 2041.
3. R. G. KULKARNI and V. U. PATIL, *J. Mater. Sci.* **17** (1982) 843.
4. R. G. KULKARNI and H. H. JOSHI, *Solid State Commun.* **43** (1985) 1005.
5. H. H. JOSHI, S. N. RAO and R. G. KULKARNI, *J. Mater. Sci. Lett.* **4** (1985) 1249.
6. C. RADHAKRISHNA MURTY, S. D. LIKHITE and P. W. SAHASRABUDHE, *Proc. Ind. Acad. Sci.* **87A** (1978) 245.
7. C. RADHAKRISHNA MURTY, S. D. LIKHITE and N. P. SASTRY, *Phil. Mag.* **23** (1971) 503.
8. V. G. PANICKER, S. N. RAO, and R. G. KULKARNI, *Solid State Commun.* **43** (1982) 647.
9. N. S. SATYA MURTHY, M. G. NATERA, S. J. YOUSSEF, R. G. BEGUM and C. M. SRIVASTAVA, *Phys. Rev.* **181** (1969) 969.
10. E. CALLEN and H. COLLEN, *J. Appl. Phys.* **36** (1965) 1140.